

A new enantiornithine specimen from the Lower Cretaceous of Las Hoyas: avifaunal diversity and life-history of a wetland Mesozoic bird

Un nuevo espécimen de enantiornita del Cretácico Inferior de Las Hoyas: diversidad avifaunística e historia vital de un ave mesozoica de humedal

Sergio M. NEBREDA¹, Luis M. CHIAPPE², Guillermo NAVALÓN³, Anusuya CHINSAMY⁴, José L. SANZ⁵, Ángela D. BUSCALIONI⁶ & Jesús MARUGÁN-LOBÓN⁷

Abstract: The Lower Cretaceous fossil site of Las Hoyas (Cuenca, Spain) has yielded the richest Cretaceous avifauna of the European continent. We describe a new fossil (MUPA-LH-33333) of an enantiornithine bird from this locality. This specimen consists of a partially articulated skeleton preserving portions of the vertebral column, both girdles and limbs, ribs and sternum; it also preserves patches of soft tissues including remigial feathers and integumentary structures belonging to the postpatagium. MUPA-LH-33333 shares dimensions and some anatomical features with the holotype of *Concornis lacustris*, a species previously described from Las Hoyas. However, the new specimen shows differences especially in the coracoid and the sternum, suggesting the presence of a different morphotype closely related to *C. lacustris*. Nevertheless, the poor preservation prevents asserting that it represents a new species. Histological evidence from its long bones indicates that it is subadult or adult and that early fast rates followed by slower and protracted cyclical phases took place during its growth, a previously unnoticed pattern in Lower Cretaceous enantiornithines. This new finding supports the hypothesis that enantiornithines regularly inhabited the Las Hoyas wetland, making this site a hotspot for enhancing our understanding of the evolution and life history of these Cretaceous birds.

Resumen: El paleohumedal del Cretácico Inferior de Las Hoyas, en Cuenca (España), contiene el registro de avifauna cretácica más rico de Europa. En este trabajo describimos un nuevo fósil (MUPA-LH-33333) de un ave enantiornita de esta localidad. Este espécimen consiste en un esqueleto parcialmente articulado que preserva partes de la columna vertebral, ambas cinturas, el esternón, las extremidades, y algunos parches de tejido blando, incluyendo plumas rémiges y estructuras integumentarias del postpatagio. MUPA-LH-33333 comparte dimensiones y detalles anatómicos con el holotipo de *Concornis lacustris*, especie previamente descrita en Las Hoyas. Sin embargo, también presenta diferencias en el coracoides y el esternón, sugiriendo la presencia de un morfotipo diferente, cercano a *C. lacustris*. Aun así, su preservación impide afirmar que sea una nueva especie. Por otro lado, la osteohistología de MUPA-LH-33333 indica que es un subadulto o un adulto, el cual contó durante su crecimiento con tasas rápidas tempranas seguidas de una fase ralentizada y cíclica, patrón no descrito anteriormente en enantiornitas. El descubrimiento de este nuevo ejemplar refuerza la hipótesis de que estos organismos habitaban el humedal de Las Hoyas regularmente, lo que hace de este yacimiento un sitio clave para aumentar nuestro conocimiento sobre la evolución e historia vital de estas aves cretácicas.

Received: 8 December 2022

Accepted: 16 April 2023

Published: 11 May 2023

Corresponding author:

Sergio M. Nebreda

sergio.martinezn@uam.es

Keywords:

Aves

Diversity

Palaeobiology

Histology

Mesozoic

Palabras-clave:

Aves

Diversidad

Paleobiología

Histología

Mesozoico

INTRODUCTION

The Early Cretaceous site of Las Hoyas (Cuenca, Spain, upper Barremian, 126–129 My, Diéguez *et al.*, 1995; Vicente & Martín-Closas, 2013) contains the most diverse and best-preserved avifauna of the Mesozoic of Europe, including the second oldest enantiornithine assemblage worldwide (Sanz *et al.*, 2016; Benito & Olivé 2022). More than 30 years of palaeontological excavations at Las Hoyas resulted in the discovery of multiple avian skeletal remains and numerous isolated

feathers (Sanz *et al.*, 2016; Marugán-Lobón & Vullo, 2016; Knoll *et al.*, 2018; Kaye *et al.*, 2019). At this site, birds represent the third most abundant group of amniotes, surpassed only by crocodylomorphs and squamates (Buscalioni *et al.*, 2016). All diagnosable avian material belongs to enantiornithines, a clade of stem birds known worldwide and throughout most of the Cretaceous (Chiappe & Walker, 2002). These fossils include the holotypes of *Iberomesornis romerali* (Sanz

et al., 1988), *Concornis lacustris* (Sanz *et al.*, 1995), *Eoalulavis hoyasi* (Sanz *et al.*, 1996), and several other specimens revealing tantalizing evidence of soft tissue micro-details (Navalón *et al.*, 2015), life-history and palaeobiology (Sanz *et al.*, 2001; Knoll *et al.*, 2018; Kaye *et al.*, 2019) of Enantiornithes.

GEOLOGICAL FRAMEWORK

Las Hoyas is a small basin contained within the upper Barremian La Huérguina Formation, which comprises a continental sedimentation in the southwestern sector of the Iberian Basin (Serranía de Cuenca, Spain; Fregeñal-Martínez *et al.*, 2017). The fossil site is composed of finely laminated limestones formed in a depositional environment interpreted as part of a freshwater, inland, and seasonal wetland that developed under a subtropical system (Buscalioni & Fregeñal-Martínez, 2010; Fregeñal-Martínez *et al.*, 2017). The Las Hoyas Basin was dated to 126–129 My based on charophytes and ostracods (Diéguez *et al.*, 1995; Vicente & Martín-Cloas, 2013; Fregeñal-Martínez *et al.*, 2017).

Previous studies have shown that the internal lithologies of the laminated limestones were ordered into a gradient of microfacies attributed to seasonality of the original environment (Buscalioni & Fregeñal-Martínez, 2010). Also, the life-history and palaeobiology of its biota was intricately linked to the palaeoenvironment, thus inherently influenced by the notable seasonality (Buscalioni & Poyato-Ariza, 2016; Buscalioni *et al.*, 2016; Martín-Abad & Fregeñal-Martínez, 2021).

MATERIALS AND METHODS

In this study, we describe a new avian specimen from Las Hoyas (MUPA-LH-33333). Preserved in two slabs (slab and counter slab), this specimen consists of a partially articulated skeleton, including portions of the axial skeleton, the pectoral and pelvic girdles, and both limbs (Fig. 1). MUPA-LH-33333 was prepared mechanically, subsequently μ CT-scanned and segmented, and histologically thin-sectioned.

Scanning information

The pectoral region of the specimen was CT-scanned at the Centro de Instrumentación Científica (University of Granada, Spain), using an Xradia 510 VERSA ZEISS microCT-scanner, comprising 2401 projections and applying the following settings: 80 kV, 7W, 6s, and 38.007 μ m voxel size for all three spatial axes. The scan data were segmented in the specialized software Avizo 9.0 to produce three-dimensional models of the best-preserved osteological elements of the pectoral girdle.

Histology

Two fragments were removed from the diaphysis of humera: section 1 from the left element and section 2 from the right one (Fig. 1). The fragments were embedded in resin and thin sections were prepared at the University of Cape Town in the Department of Biological Sciences following the methodology of Chinsamy and Raath (1992). The thin sections were studied using a Zeiss Axio Lab.A1 petrographic microscope and photo-

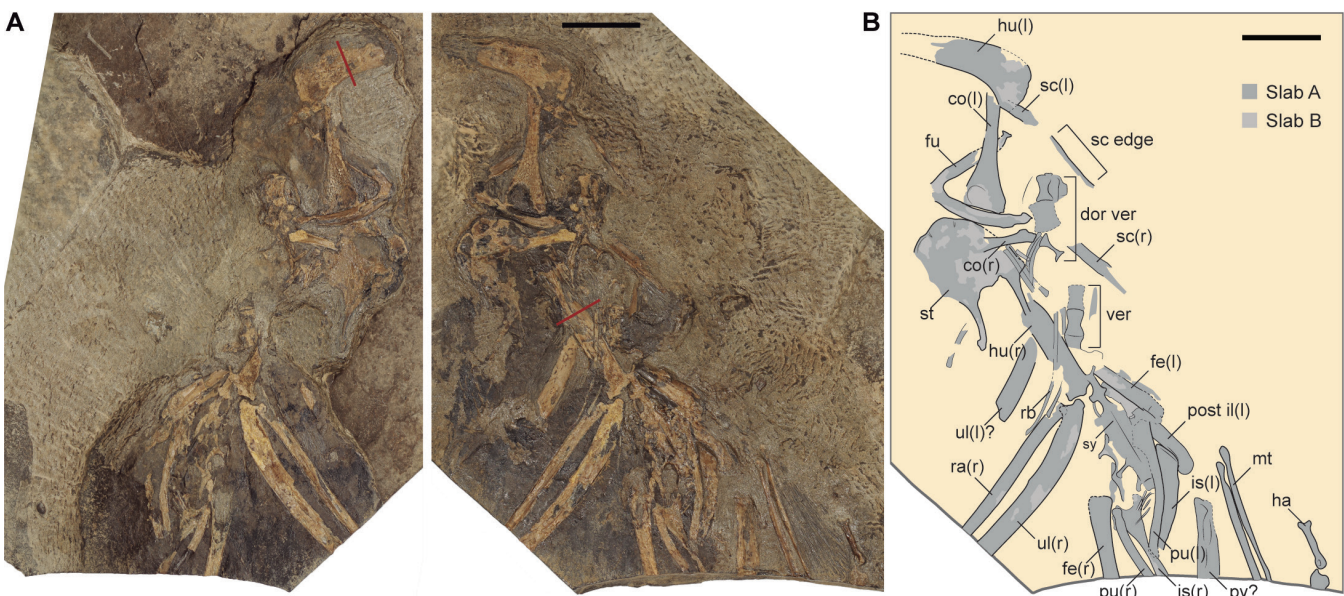


Figure 1. Slab (slab A, right) and counterslab (slab B, left) of the new enantiornithine specimen from the Las Hoyas fossil site (Early Cretaceous, Cuenca, Spain) MUPA-LH-33333, showing its skeletal and soft tissue remains. Red lines indicate where the thin sections were obtained. Abbreviations: **co**, coracoid; **fe**, femur; **fu**, furcula; **ha**, hallux; **hu**, humerus; **is**, ischium; **mt**, metatarsus; **pu**, pubis; **py**, pygostyle; **ra**, radius; **rb**, rib; **sc**, scapula; **st**, sternum; **sy**, synsacrum; **ul**, ulna; **ver**, vertebra; scale bar = 10 mm.

micrographs were taken using an Axiocam 208 Color camera.

Data availability

Three-dimensional digital mesh for the furcula, the coracoid, and the remains of the sternum of MUPA-LH-33333, and original μ -CT stack of the scanned part of the fossil are available from the Morphosource Repository: <https://www.morphosource.org/projects/000502754?locale=en>.

RESULTS

Anatomical description

The anatomical terminology follows [Baumel *et al.* \(1993\)](#). Based on measurements from the coracoid and furcular rami, MUPA-LH-33333, represents a bird close in size to the holotypes of *Concornis lacustris* and *Eoalulavis hoyasi*. Coracoid and furcular rami are 91.6% and 89% of the lengths of these bones in *C. lacustris*; 98% of the length of both elements in *E. hoyasi*, thus falling in the upper end of the size range of the known avian remains from Las Hoyas (Tab. 1). Histological sampling of the humeral compacta documents the presence of poorly vascularized parallel fibred bone subperiosteally, which, together with the completeness of the sternum, suggests that MUPA-LH-33333 corresponds to a subadult or an adult individual (see Histology section below).

The skeleton of MUPA-LH-33333 is partially articulated and slightly taphonomically twisted, showing the forelimbs overlapping and nearly in line with the axial skeleton and the pelvic region (Fig. 1). The fossil is preserved along two different planes. The anterior region is placed at the upper level of the layer, showing elements with remarkable taphonomic alterations (both humeri are fractured) and displaced from their original anatomical position. The posterior region is placed at the lower level of the layer and is better preserved, even showing feathers in its anatomical position (see Soft tissues section). Since the skeleton is twisted, the elements of the skeleton are not preserved in the same anatomical views; two of the three dorsal vertebrae, which are articulated, are preserved in lateral view, but the third is in ventral view, and in the slab B the furcula is in ventral view but the sternum is dorsally exposed (Fig. 2).

Axial skeleton

The three anterior dorsal vertebrae are preserved adjacent to the omal end of the right furcular ramus and positioned parallel to the left coracoid (Fig. 1; Supplementary Information Fig. S1A). The first vertebra shows a large oval recess laterally excavating its centrum, identified as the pleurocel, as is typical (albeit highly variable in size) of enantiornithines and other stem birds ([Chiappe & Walker, 2002](#)). Dorsal to this recess,

Table 1. Selected measurements of MUPA-LH-33333 and other avian specimens from Las Hoyas, including *Iberomesornis romerali* ([Sanz *et al.*, 1988](#)), *Concornis lacustris* ([Sanz *et al.*, 1995](#)), *Eoalulavis hoyasi* ([Sanz *et al.*, 1996](#)), an enantiornithine hatchling ([Knoll *et al.*, 2018](#)), the three individuals contained in a pellet ([Sanz *et al.*, 2001](#)), and an undescribed isolated pectoral region. All measurements are in mm.

	MUPA-LH-33333	<i>Iberomesornis romerali</i> (MUPA-LH-022)	<i>Concornis lacustris</i> (MUPA-LH-2814)	<i>Eoalulavis hoyasi</i> (MUPA-LH-13500)	Hatchling (MUPA-LH-26189)	Pellet ind.1 (MUPA-LH-11386)	Pellet ind.2 (MUPA-LH-11386)	Pellet ind.3 (MUPA-LH-11386)	MUPA-LH-16683
Coracoid	15.05	9.82	15.73	16.52	5.4	8.76	-	-	13.24
Furcular rami	12.51	7	13.31	11.95	4.99	7.52	-	-	-
Humerus	27.53	17.62	32.69	27.12	10.6	16.04	-	-	25.45
Ulna	-	18.79	25.05	30.39	9.9	-	-	-	-
Radius	-	16.93	21.86	27.45	8.7	-	-	-	-
Femur	-	19.07	24.04	-	10.8	18.19	18.07	-	-
Tibiotarsus	-	19.45	34.71	-	-	-	21.71	-	-
Tarsometatarsus	-	11.63	21	-	-	13.3	16.2	10.83	-
Phalanx 1 Toe Digit I	5.81	3.28	3.54	-	-	3.19	-	-	-

there is a round structure that is likely the parapophysis (Supplementary Information Fig. S1A), located centrally as characteristic of Enantiornithes ([Chiappe & Walker, 2002](#)). The second vertebra appears to have a large, craniocaudally rectangular spinous process. The third vertebra displays a mediolaterally compressed ventral margin, presumably accentuated by the lateral excavations of the centrum (left and right lateral fossae; Supplementary Information Fig. S1A). The well-preserved margins of the cranial and caudal articular surfaces of this centrum indicate that the vertebra was amphiplatyan. A few damaged remnants of other dorsal vertebrae are preserved caudal to these anterior dorsals and cranial to the synsacrum. These remnants, however, barely allow any anatomical information.

The synsacrum (16.46 mm long) is exposed ventrally and it appears to have been composed of seven fused vertebrae (Supplementary Information Fig. S1B), a number that falls within the range known for Enantiornithes ([Liu *et al.*, 2019](#)). This number is equivalent to the one reported for *Protopteryx* ([Zhang & Zhou, 2000](#); [Chiappe *et al.*, 2019b](#)), *Pengornis* ([Zhou *et al.*, 2008](#)), *Rapaxavis* ([O'Connor *et al.*, 2011](#)), *Bohaiornis*, ([Hu *et al.*, 2011](#)), and *Parabohaiornis* ([Wang *et al.*, 2014a](#)). The cranialmost two vertebrae of the synsacrum are craniocaudally longer than the remaining ones. The third to fifth vertebrae appear to be wider in ventral view than the others, and the caudalmost two (sixth and seventh) are narrower and shorter than the rest. While the transverse processes of these

synsacral vertebrae are not well-preserved, it is clear that the transverse processes of the sixth and seventh synsacral vertebrae are longer than the rest, and those of the caudalmost one is more caudally angled than those of cranial synsacral vertebrae (Fig. 1; Supplementary Information Fig. S1B), a condition known for enantiornithines (Chiappe *et al.*, 2019a; Liu *et al.*, 2019). The ventral surface of the synsacrum bears a shallow groove, which seems to be limited to the third through seventh vertebrae, as in *Rapaxavis* and *Zhouornis*, albeit less pronounced (O'Connor *et al.*, 2011; Zhang *et al.*, 2014) (Fig. 1; Supplementary Information Fig. S1B). Such a groove has been reported

on a number of enantiornithines and its extension is variable: *Piscivorenanantiornis* (Wang & Zhou, 2017) has a groove from the fourth to the last sacral vertebra; and in *Yuanjiawaornis* (Hu *et al.*, 2015), it spans along the whole length of the ventral surface of the synsacrum. At least three free caudal vertebrae cranial to the pygostyle are visible and in articulation with the synsacrum. These are craniocaudally shortened compared to the synsacral vertebrae and bear elongated and slender transverse processes. Any remaining free caudals are covered by the left pubis (Supplementary Information Fig. S1B). Finally, a large bone tentatively identified as the pygostyle is preserved

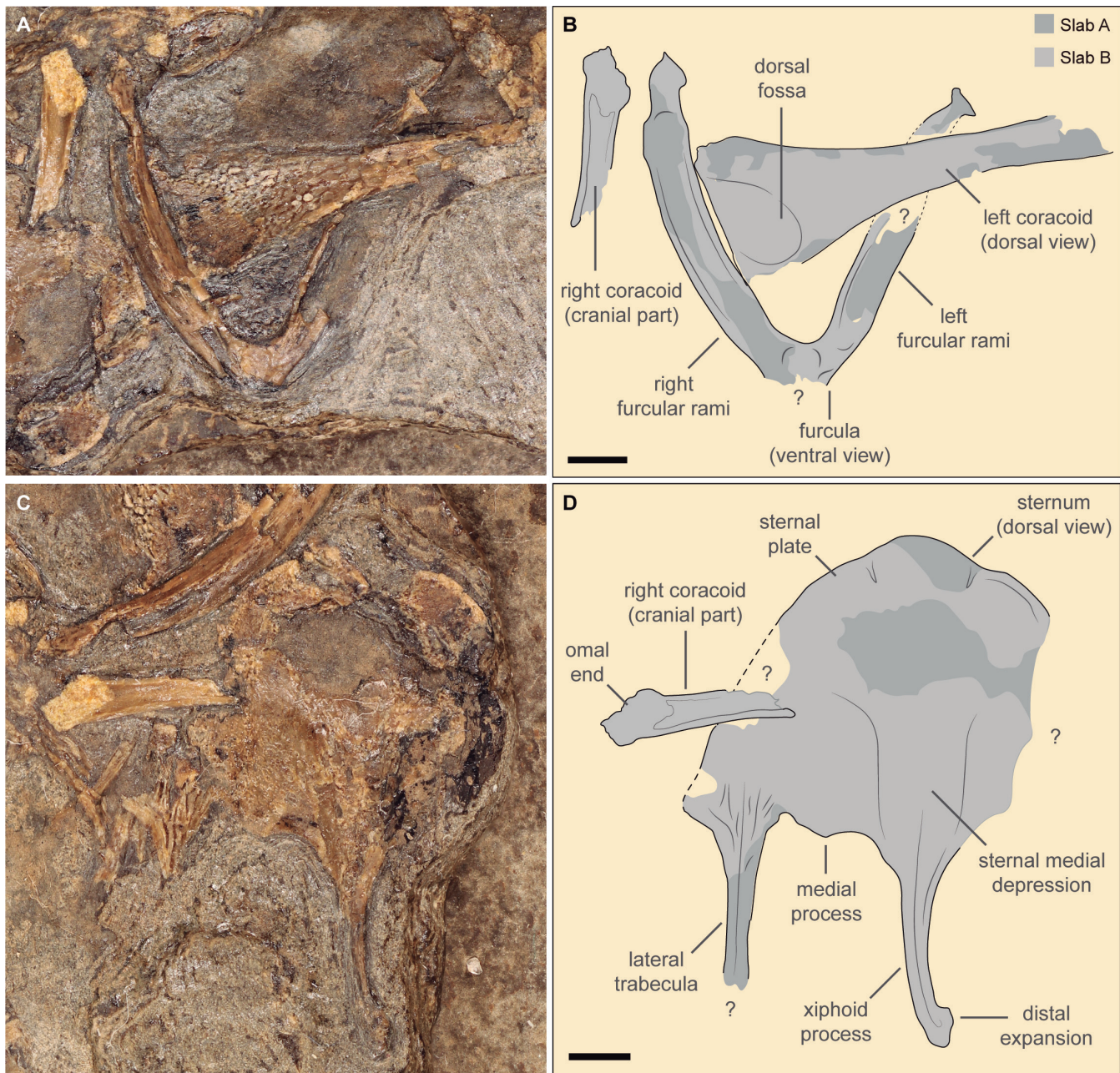


Figure 2. Anatomical details of the pectoral region remains of MUPA-LH-33333 preserved on slab B. **A**, Picture of the pectoral girdle; **B**, interpretative drawing of a composite through camera lucida of the remains preserved on both slabs; **C**, picture of the sternum; **D**, interpretative drawing of a composite through camera lucida of the remains preserved on both slabs. Question marks indicate areas where the bone was not preserved; scale bars = 2 mm.

disarticulated from the axial skeleton, at the edge of the slab A, between the pelvic region and some bones of the hindlimb.

Pectoral girdle & limb

The left coracoid (15.05 mm long) is relatively well-preserved. It is strut-like, long and relatively slender (Figs. 2, 3). Its maximum length/width ratio of 2.56 is greater than in some enantiornithines (e.g., length/width ratio is 1.8 and 2.2 in *Bohaiornis* and *Eoenantiornis*, respectively) but lesser than other species (e.g., 2.74 in *Concornis*, 2.98 in *Eoalulavis*, and 3.43 in *Enantiornis*).

The dorsal surface of the sternal portion of the coracoid bears a distinct sternocoracoidal fossa, common to most enantiornithines (Chiappe & Walker, 2002). The medial and lateral margins of this bone are straight and slightly convex, respectively (Figs. 2, 3), as in *Iberomesornis* (Sanz *et al.*, 1988, 2016), *Longipteryx* (Zhang *et al.*, 2001), *Rapaxavis* (Morschhauser *et al.*, 2009), *Bohaiornis* (Hu *et al.*, 2011), and many other enantiornithines (Chiappe & Walker, 2002). The shape of the sternal margin of the coracoid varies among enantiornithines, from straight to strongly concave (e.g., Chiappe & Walker, 2002; Chiappe *et al.*, 2019a; Liu *et al.*, 2022). The morphology of this

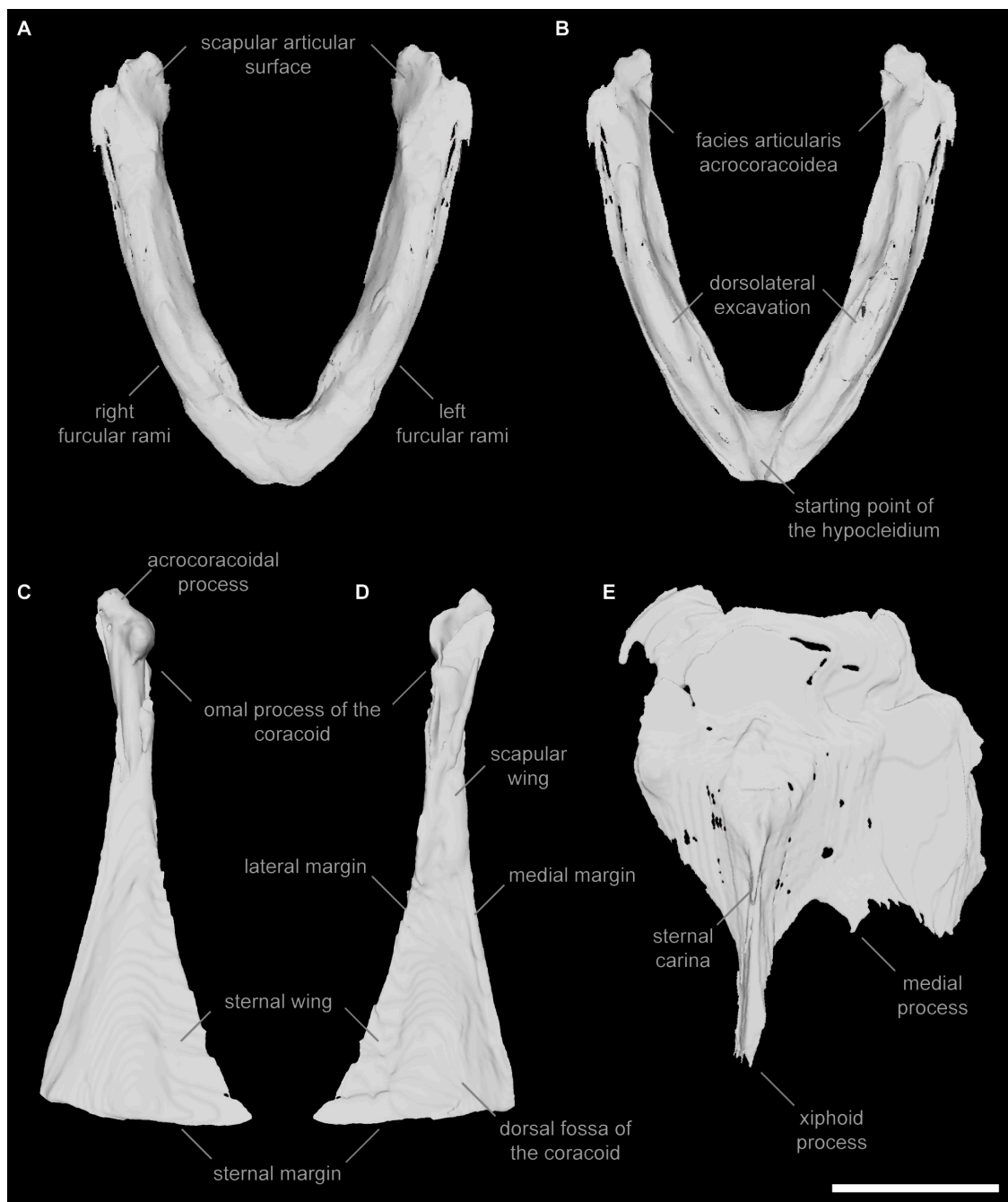


Figure 3. A–B, Digital reconstructions of the furcula; A, ventral; B, dorsal; C–E, the left coracoid; C, ventral; D, dorsal views; E, sternum, showing some details of their anatomy. All structures are scaled; scale bar = 5 mm.

margin in MUPA-LH-33333 (5.87 mm wide) resembles the straight margin of *Concornis lacustris* (Sanz *et al.*, 1995), although it is more obliquely oriented in the latter (Fig. 6). The omal end of the right coracoid, presumably exposed in lateral view, shows the dorsally slanted outline typical of enantiornithines (Chiappe & Walker, 2002).

Portions of a V-shaped furcula are exposed dorsally in slab A and ventrally in slab B (Figs. 1, 2). The interclavicular angle is approximately 55°, as in *Junornis* (Liu *et al.*, 2017), falling within the range of most enantiornithines (e.g., *Longirostravis* = 50°, and *Bohaiornis*, *Concornis* and *Sulcavis* = 60°). The distance between the tips of the rami reaches a maximum separation of 11.64 mm. In dorsal view, the rami (~12.5 mm long) are slightly curved. In transverse section, it has the L-shape characteristic of enantiornithines (Chiappe & Walker, 2002), in which the ventral margin is wider than the dorsal margin and both are separated by a wide excavation that runs through most of the dorsolateral surface of the ramus (Fig. 3).

A portion of the sternum, representing most of the left half, is preserved in dorsal view in slab B (where it is better preserved). The cranial margin of the sternum appears to be rounded (Fig. 2). Caudally, this bone bears an elongated xiphoid process (approximately 82% of the craniocaudal length of the sternal plate), that is gently expanded distally. This process is taphonomically deformed so that it curves towards the right side (Fig. 2). Portions of the left lateral trabecula are also visible, and most of its length can be pieced together from portions preserved on both slabs (however, its distal end is missing). It is caudally directed, nearly but not completely parallel to the xiphoid process, similar to *Cathayornis* (Zhou & Hou, 2002), *Rapaxavis* (O'Connor *et al.*, 2011) and *Dunhuangia* (Wang *et al.*, 2015). There appears to be a small xiphoid process on the lateral margin proximal to the lateral trabeculae similar to *Cathayornis* (Zhou & Hou, 2002), but this portion is not completely preserved and should therefore be treated with caution. There is a minimally developed medial process between the lateral trabecula and xiphoid process, which is equidistant from both the former processes, as in many other enantiornithines, e.g., *Bohaiornis*, *Zhouornis*, *Vescornis* and *Cathayornis* (Zhou & Hou, 2002; Zhang *et al.*, 2004, 2014; Wang *et al.*, 2014a) (Fig. 2). Cranial to the xiphoid, there is a symmetrical depression on the dorsal surface of the sternum. CT volumes revealed a slightly developed carina on the ventral surface of this area, thus mirroring the above-mentioned dorsal depression. This sternal carina extends from the caudal half of the sternal plate to the cranial third of the xiphoid process (Fig. 3). However, we do not have clear evidence to indicate that the complete carina is preserved.

The proximal portion of the left humerus is preserved next to the left coracoid; its preserved portion (preserved length = 12.35 mm, maximum width = 6.05

mm), includes the entire length of the deltopectoral crest (11 mm long; Supplementary Information Fig. S1C). The distal half of the right humerus (preserved length = 18.27 mm) is preserved diagonally between the furcula and the synsacrum, yet it is too poorly preserved to provide any anatomical information. This element is articulated to the ulna and radius, of which approximately the proximal two-thirds are preserved (preserved ulnar length = 22.48 mm; preserved radial length = 19.33 mm). The proximal end of the ulna bears a well-developed olecranon, which projects beyond the cotylar surface. The ulnar shaft is slightly curved, as in other enantiornithines and early birds, and its caudal margin does not show any evidence of remigial papillae although this region is very poorly preserved. The radius is straight, and its midshaft width is about 65% that of the ulna at roughly mid-point (Supplementary Information Fig. S1D).

Pelvic girdle & limb

Fragments of the three pelvic bones are preserved surrounding the synsacrum (Supplementary Information Fig. S1E). The most reliably identifiable portion of the ilium is the postacetabular wing of the right element. It is slender as is typical of enantiornithines, gently curved (medially concave), and with a blunt end (Fig. 1). The pubes are slender and gently curved medially; portions of the shafts of both sides are preserved. The mid-portion of the left pubis indicates that the ventral surface of this bone was rounded and similar to that of *Concornis lacustris*. The ischia are belt-like but poorly preserved, running parallelly to the pubes; the left ischium appears to have a distinct proximocaudal process. In all, the morphology of the ischia is also comparable to that of *C. lacustris*.

Very little anatomical information is available for the hindlimb. The left femur is in near articulation with its acetabulum. The proximal portion of the right femur is also in near-articulation with its acetabulum. Two metatarsals are preserved parallel to a tentatively identified pygostyle (Fig. 1; Supplementary Information Fig. S1F). Their distal trochleae are expanded but too poorly exposed to provide any additional information. We interpret the most projected element as metatarsal III based on their relative position, and the other as metatarsal II given that it is comparable in width to the latter (enantiornithine metatarsi IV are often much slenderer than their counterparts; Chiappe & Walker, 2002). The absence of metatarsal IV and the connection between the two preserved metatarsals suggest that these bones were unfused to one another, at least through the distal portion of the metatarsus. The degree of fusion in the proximal portion of the metatarsal is unknown as it is missing. There is a long and slender, isolated non-ungual phalanx (5.81 mm long) articulated to what appears to be the proximal region of an unguis phalanx (Fig. 1; Supplementary Information Fig. S1F). The distal



Figure 4. Soft tissues preserved in MUPA-LH-33333. **A**, Details of the soft tissue of the wing preserving at least four remigial feathers (black arrows) inserted into the postpatagium through their calami (yellow arrows), and attached possibly by remains of indeterminable integumentary structures (red arrow); **B**, interpretative drawing showing the rachis of the remigial feathers (black), the postpatagium (pink), the vanes of the flight feathers (light brown) and a patch of unknown soft tissue; scale bar = 5 mm.

end of the non-ungual phalanx bears a well-defined articular facet, and its side is recessed by a collateral ligamental pit. These two phalanges are interpreted as belonging to the hallux, with a morphology similar to that of the enantiornithine *Soroavisaurus australis* (Chiappe, 1993).

Soft tissues

MUPA-LH-33333 preserves remains of soft tissues as brownish-to-blackish carbonized structures in several regions of the specimen, particularly around the sternum and associated with the ulna (Fig. 4). The soft tissue near the sternum appears to be fiber-like disorganized structures that resemble feathers (Fig. 4A). These structures can be observed in photographs taken prior to mechanical preparation, which unfortunately destroyed most of them. The soft tissues below the ulna appear to be preserved in their original anatomical position (Fig. 4B): four-five remigial feathers are observed as dark structures associated with a grey-to-brown halo of soft tissue similar to the postpatagium observed in another Las Hoyas specimen (Navalón *et al.*, 2015). The postpatagium appears to have a sinusoidal caudal outline scattered by the calami of the secondary remiges, which are also preserved as carbonaceous remains. A bundle of fibers with a serially striated pattern can be observed in association with some of these calami (red arrow in Fig. 4B). These structures have been interpreted as remains of the system of tendons, muscles and ligaments associated with the calami of flight feathers (Navalón *et al.*, 2015). Feather vanes are poorly preserved, but some barbs can be observed.

Histology

Of the two sections prepared, one of them was quite crushed (section 2), whereas the other section although just a tiny fragment of the bone wall, was better preserved (section 1). The latter section (Fig. 5A–5B) shows that the bone wall comprised of a cyclically formed, triple layer of bone tissue: two deposits of parallel fibred bone with a relatively evenly distributed osteocyte lacunae, and fibres arranged orthogonally as indicated by the birefringence. Internal to this outer band of tissue (which is likely the outer circumferential layer), there is a region with more woven type of bone tissue wherein the osteocyte lacunae are plumper and haphazardly arranged, which suggests a faster rate of bone formation (Fig. 5). The perimedullary region is not preserved.

The presence of the cyclically formed, triple layer outermost region of more organized osteocyte lacunae suggests that MUPA-LH-33333 is a mature individual, that had passed its most rapid phase of growth. The lack of vascularization could be a preservation or sampling bias (since the sample is just a small flake of bone), or it could be that the earliest most rapidly formed bone has been resorbed. Despite being crushed, and therefore sectioned in different planes, the second thin section (Fig. 5C–5E) reveals similar histological features as described in the first section, *i.e.*, an outer more slowly formed triple layer of bone tissue, and a more disorganized bone tissue located centrally which has a few inconspicuous vascular canals (Fig. 5C). The latter tissue is likely displaced fragments from elsewhere in the bone shaft. A single circumferentially organized

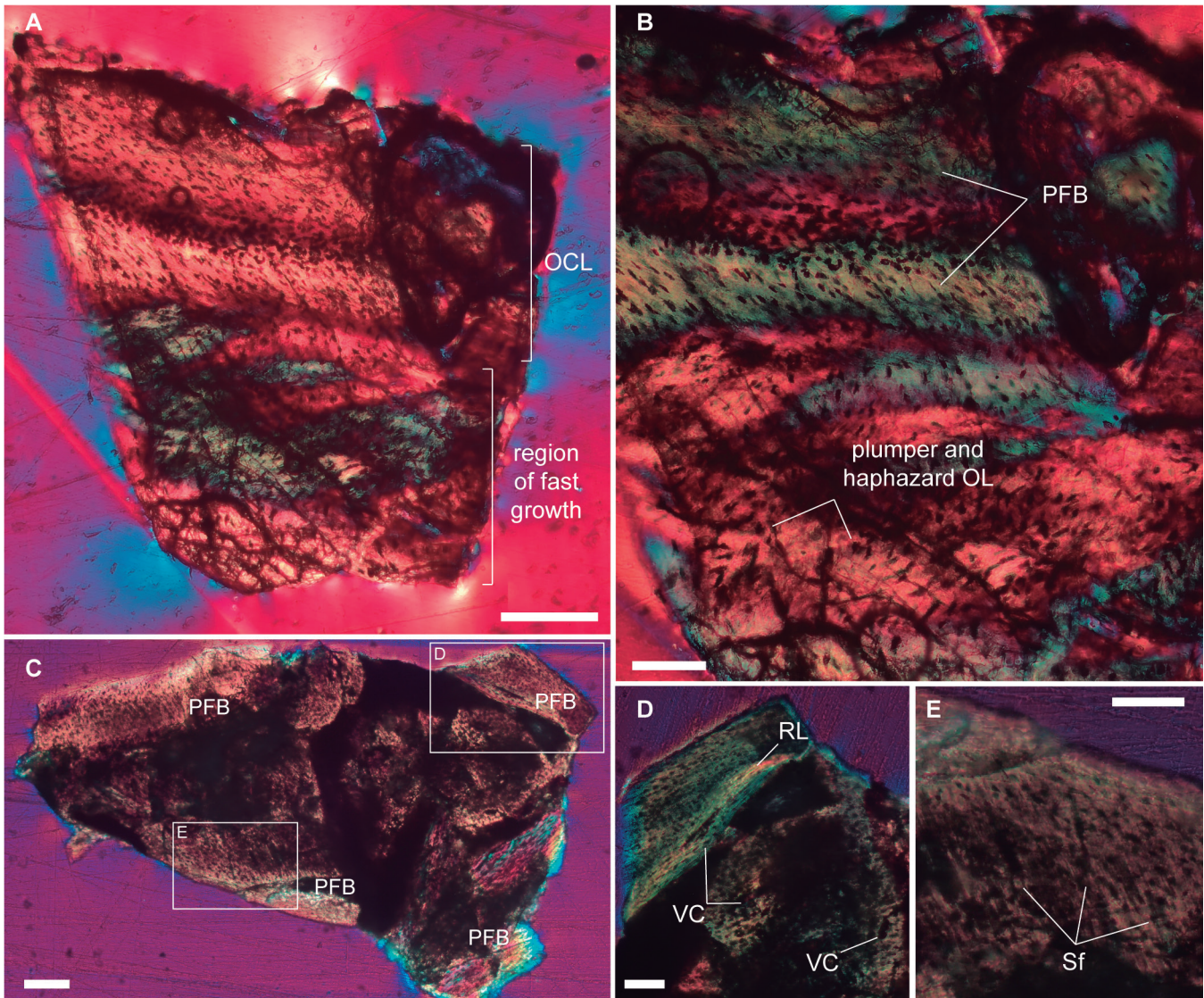


Figure 5. Micrographs of the thin sections of the left and right humeri of MUPA-LH-33333 taken under polarised light with a $\frac{1}{4}$ lambda plate. **A**, General view of section 1 (left humerus), showing a triple layered outer circumferential layer (**OCL**) internal to which is a region of more woven textured bone with disorganised osteocyte lacunae that suggests a faster rate of bone formation; scale bar = 200 μ m; **B**, higher magnification of (**A**) showing the parallel fibred bone (**PFB**) within the OCL, separated by a narrow layer with more densely packed osteocyte lacunae, as well as the deeper cortex tissue with more haphazardly organised osteocyte lacunae (**OL**); scale bar = 100 μ m; **C**, general view of the crushed section 2 (right humerus) showing the parallel fibred bone of the OCL, as well as the centrally located more disorganised bone tissue; scale bar = 200 μ m; **D**, higher magnification of the framed region in (**C**) showing a single vascular canal (**VC**) in the secondarily formed lamellar textured bone tissue located beneath a resorption line (**RL**); scale bar = 100 μ m; **E**, higher magnification of the framed region in (**C**) showing the radially organised vascular canals and abundant Sharpey's fibres (**Sf**); scale bar = 100 μ m.

vascular canal is visible within a narrow strip of what appears to be secondarily deposited lamellar bone tissue formed under a resorption line. There are several Sharpey's fibres associated with radially organized vascular canals in parts of the outer compacta (Fig. 5E), which suggests that they are areas of muscle attachment.

DISCUSSION

MUPA-LH-33333 bears several postcranial anatomical features that unambiguously identify it as an enantiornithine, like other avian remains from the fossil site of

Las Hoyas. While slightly smaller in overall size (~89–92% based on coracoid and furcular rami lengths), MUPA-LH-33333 shares some anatomical features with the holotype of *Concornis lacustris* (Sanz *et al.*, 1995). Namely, these two specimens have a long and relatively slender coracoid with a nearly straight sternal margin, a rounded cranial margin of the sternum, and a robust furcula with a similar interclavicular angle (55°). However, the lateral border of the coracoid in MUPA-LH-33333 is not strongly convex as in the holotype of *C. lacustris* (Sanz *et al.*, 1995), and the lateral trabecula of the sternum is thinner and less laterally angled in MUPA-LH-33333 (Fig. 6). In addition, the

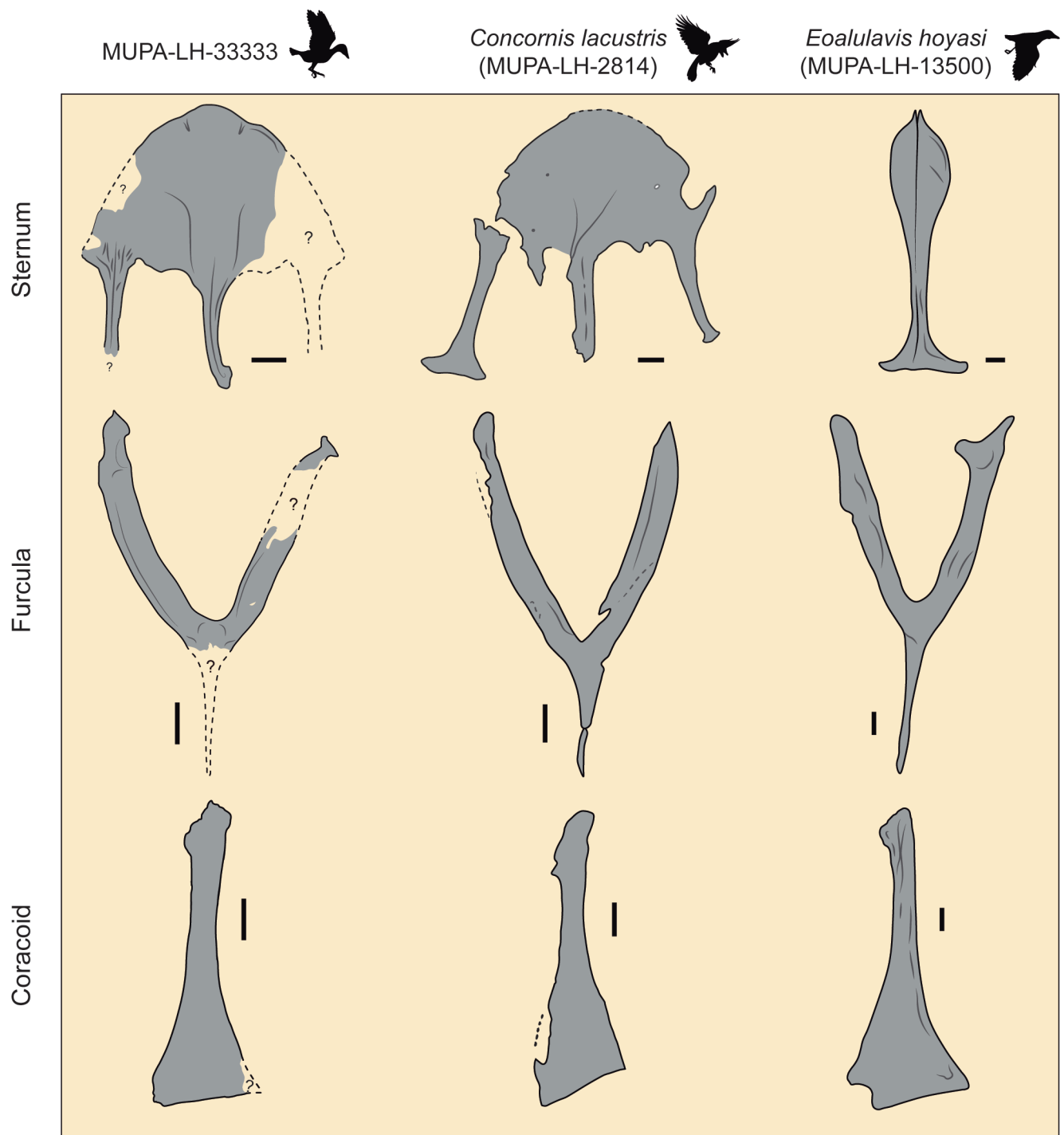


Figure 6. Comparisons between the pectoral girdle and sternum of MUPA-LH-33333 and the holotypes of *Concornis lacustris* (MUPA-LH-2814) and *Eoalulavis hoyasi* (MUPA-LH-13500). Notice the similarity between the new specimen and *C. lacustris*; scale bars = 2 mm.

medial process of the sternum is more developed in the holotype of *C. lacustris*, and this specimen shows cranio-lateral processes and paracoracoidal ossifications on both sides of the sternum (Sanz et al., 2016) that appear absent in MUPA-LH-33333 (however, given the incompleteness of the specimen, these latter differences may be preservational). Finally, the phalanx identified as belonging to the hallux is thinner than that of the *C. lacustris* holotype and significantly (45%) longer, but we cannot rule out that this could be another digit.

The other species previously described from Las Hoyas, *I. romerali* (Sanz et al., 1988) and *E. hoyasi* (Sanz et al., 1996), exhibit clear morphological differences when compared to MUPA-LH-33333. *Iberomesornis romerali* is much smaller, and although the holotype is probably a juvenile (Sanz et al., 2016; Cubo et al., 2022), it bears a concave lateral margin of the coracoid, among other distinctive characters that are absent in MUPA-LH-33333 (e.g., furcular rami slightly curved medially along omal half, metatarsal

length subequal). *Eoalulavis hoyasi*, is similar in size to MUPA-LH-33333 (around 98%), but this taxon exhibits several unique anatomical features, such as a spear-shaped sternum with a foot-like caudal expansion, and a much more elongated and slender coracoid with a strongly convex border that expands broadly towards the sternal margin (Fig. 6). This set of morphologies appears to indicate that MUPA-LH-33333 is different from the species previously described from Las Hoyas. However, the poor preservation of MUPA-LH-33333 and the lack of information on important morphologies, hamper comparisons and restrain us from erecting a new species.

MUPA-LH-33333 increases the diversity of the Las Hoyas avifauna and, together with the other avian remains, confirms that the presence of enantiornithine birds in this wetland is not circumstantial, as documented by the abundance of this group in relation to other tetrapod groups (e.g., non-avian dinosaurs, pterosaurs, or mammals). The anatomical completeness and the twisted skeleton of MUPA-LH-33333 suggests that the individual was not transported. In actuataphonomical experiments, avian carcasses deposited in tanks of standing water become twisted and frequently disarticulated during decay (Cambra-Moo *et al.*, 2008). Because twisted avian skeletons do not presuppose transport, we assume that MUPA-LH-33333 is an autochthonous fossil likely dead and decayed in water or nearby. Moreover, the presence of several remains of non-adult individuals suggests that the enantiornithine birds from Las Hoyas were breeding in the wetland (Sanz *et al.*, 2001, 2016; Knoll *et al.*, 2018; Kaye *et al.*, 2019), especially due to the existence of MUPA-LH-26189, a perinate chick with a largely cartilaginous sternum, insufficient to provide anchor to the wing muscles (Knoll *et al.*, 2018). Such observation led the authors to assume that this chick was not able to fly precociously. Altogether, this evidence indicates that enantiornithines are largely demic components of the Las Hoyas fossil assemblages, representing a substantial component of the original fauna and breeders of the wetland.

Although MUPA-LH-33333 still shows important differences, especially in the shape of the coracoid and the sternum, it is evident that, comparing the new specimen within the context of the Las Hoyas avifauna, morphological similarity exists between this specimen and the holotype of *C. lacustris*. Considering this, close morphotypes or even intraspecific variability (e.g., dimorphism, polymorphism, and specially ontogeny given the osteohistological differences) cannot be ruled out. Given the rich fossil record of birds and the short time recorded at the Las Hoyas fossil site, it is likely that this record is capturing this type of variability, as is the case for fishes, arthropods, and plants (Buscalioni & Fregenal-Martínez, 2010; Buscalioni & Poyato-Ariza, 2016; Buscalioni *et al.*, 2016; Martín-Abad & Fregenal-Martínez, 2021). Intraspecific variability has been widely studied in the Early Cretaceous *Confucius*

sornis sanctus (Chiappe *et al.*, 2008; Marugán-Lobón *et al.*, 2011; Chinsamy *et al.*, 2013; Marugán-Lobón & Chiappe, 2022)—these studies have documented variation in size (across a growth series), sexual dimorphism, and allometry within this Chinese bird species. However, given that the timespan represented by the limestones of Las Hoyas and the original biota recovered therein—estimated in thousands or tens of thousands of years (Buscalioni & Fregenal-Martínez, 2010) is significantly narrower than that the time interval containing specimens of *Confuciusornis*, the presence of close morphotypes can help to better understand how diversity works in Mesozoic birds together with speciation events and microevolutionary dynamics.

As mentioned above, the seasonality and cyclicity of the wetland have been linked to both changes in the fossil assemblages and is also evident in the life-history attributes of fishes, arthropods and plants inhabiting the wetland during different seasons (Buscalioni & Fregenal-Martínez, 2010; Buscalioni & Poyato-Ariza, 2016; Buscalioni *et al.*, 2016; Martín-Abad & Fregenal-Martínez, 2021). Like other enantiornithine birds studied osteohistologically, it appears that this bird experienced rapid growth during early stages of ontogeny, and that during later ontogeny they experienced cyclical slow growth for protracted periods (Chinsamy *et al.*, 1995, 2019; Cambra-Moo *et al.*, 2006; Zhang *et al.*, 2013; Wang *et al.*, 2014b; Atterholt *et al.*, 2021). It is possible that the cyclical pattern of bone deposition observed in the outer cortex may have been linked to the particular dynamics of the wetland, such as seasonality (Buscalioni & Fregenal-Martínez, 2010; Buscalioni *et al.*, 2016) and food availability (Buscalioni *et al.*, 2016; Barrios-de Pedro *et al.*, 2020).

The osteohistology of MUPA-LH-33333 suggests that it is a bird that passed its most rapid stage of growth, and that it was at a stage of slower, protracted growth at the time of its death, being a subadult or an adult with a different growth pattern. Interestingly, unlike many other adult enantiornithine birds, including *C. lacustris* (Cambra-Moo *et al.*, 2006), no lines of arrested growth were observed in the outer parts of the compacta (*i.e.*, the outer circumferential layer), which directly indicates that although growth was slow, bone deposition had not ceased periodically. This could mean that it had a unique growth strategy as compared to other mature enantiornithine birds, or perhaps we are seeing part of a cyclical growth pattern, like in *Mirarce* (Atterholt *et al.*, 2021), or simply that it had not yet formed its first line of arrested growth. It is also worth mentioning that the distinctive birefringence pattern observed in MUPA-LH-33333 has not previously been observed in other enantiornithine birds.

MUPA-LH-33333 also provides important information about the palaeobiology of these basal birds. While the missing elements of its skeleton prevent an accurate estimate of the flight performance of this specimen, the presence of soft tissues such as flight feathers and integuments structurally similar to those of the wing of

MUPA-LH-31444 (Navalón *et al.*, 2015) supports previous claims related to the sophisticated flight performance of enantiornithines, due to the similarity to these structures in modern birds (Liu *et al.*, 2019; Chiappe *et al.*, 2019a, 2019b). In fact, the overall similar proportions of MUPA-LH-33333 to those of the holotype of *C. lacustris* and *E. hoyasi*, suggest that this bird may have also been capable of bounding flight (Serrano *et al.*, 2018).

Supplementary information. Figure S1 is available at the Spanish Journal of Palaeontology web-site (<https://sepaleontologia.es/spanish-journal-palaeontology/>) linked to the corresponding contribution. Scan data is archived in the online repository MorphoSource: <https://www.morphosource.org/projects/000502754?locale=en>.

Figure S1. Anatomical details of different skeletal regions of MUPA-LH-33333. **A**, Thoracic vertebrae; **B**, synsacrum; **C**, humeral head of the left humerus; **D**, ulna and radius; **E**, pelvic region; and **F**, metatarsus and hallux.

Author contributions. SMN conceived the study. SMN, LMC, GN, ADB and JM-L studied the anatomy. SMN segmented the CT-scans. AC did the thin sections and studied the osteohistology. All the authors wrote the manuscript.

Competing interest. The authors declare no competing interests.

Funding. This study has been funded by the 2021 call of the grant program 'Ayudas a Jóvenes Investigadores de la Sociedad Española de Paleontología'. SMN is supported by a FPI-UAM 2019 predoctoral grant from the Universidad Autónoma de Madrid. SMN, GN, ADB and JM-L are supported by the PID2019-105546GB-I00 project from the Ministerio de Ciencia, e Innovación de España. GN is funded by UKRI grant MR/S032177/1. This work is a contribution of the CIPb-UAM research group.

Author details. Sergio M. Nebreda^{1,2}, Luis M. Chiappe³, Guillermo Navalón^{1,2,4}, Anusuya Chinsamy⁵, José L. Sanz^{1,6}, Ángela D. Buscalioni^{1,2}, Jesús Marugán-Lobón^{1,2}. ¹Unidad de Paleontología, Dpto. Biología, Universidad Autónoma de Madrid, 28049 Cantoblanco (Madrid), Spain; ²Centro para la Integración en Paleobiología, Universidad Autónoma de Madrid, 28049 Cantoblanco (Madrid), Spain; sergio.martinez@uam.es, angela.delgado@uam.es, jesus.marugan@uam.es; ³Dinosaur Institute, Natural History Museum of Los Angeles County, Los Angeles, CA, USA; lchiappe@nhm.org; ⁴Department of Earth Sciences, University of Cambridge, Cambridge, UK; gn315@cam.ac.uk; ⁵Department of Biological Sciences, University of Cape Town, Private Bag X3, Rondebosch 7701, South Africa; anusuya.chinsamy-turan@uct.ac.za; ⁶Real Academia de Ciencias Exactas, Físicas y Naturales, c/ de Valverde, 24, 28004 Madrid, Spain; dinoproyecto@gmail.com

Acknowledgements. The authors would like to acknowledge Mercedes Llandres from the Museo Paleontológico de Castilla-La Mancha for the access to the specimen, Maureen Walsh from the Dinosaur Institute of the Natural History Museum of Los Angeles County for the preparation and curation of the specimen, Stephanie Abramowicz also from the Dinosaur Institute for the photographs and illustrations of the specimen, and Fátima Linares from the Microscopy and Microtomography Unit of the Centro de Instrumentación Científica (Universidad de Granada) for its help with the

microCT-scans. Authors would like to also thank the reviewers of the manuscript, Jessie Atterholt (Western University of Health Sciences) and Jingmai K O'Connor (Field Museum of Natural History), for their comments which helped to improve the work.

REFERENCES

- Atterholt, J., Poust, A. W., Erickson, G. M., & O'Connor, J. K. (2021). Intraskelletal Osteohistovariability Reveals Complex Growth Strategies in a Late Cretaceous Enantiornithine. *Frontiers in Earth Science*, 9, 640220. doi: [10.3389/feart.2021.640220](https://doi.org/10.3389/feart.2021.640220)
- Barrios-de Pedro, S., Rogers, K. M., Alcorlo, P., & Buscalioni, A. D. (2020). Food web reconstruction through isotopic compositions of fossil faeces: Insights into the ecology of a late Barremian freshwater ecosystem (Las Hoyas, Cuenca, Spain). *Cretaceous Research*, 108, 104343. doi: [10.1016/j.cretres.2019.104343](https://doi.org/10.1016/j.cretres.2019.104343)
- Baumel, J. J., King, A. S., Breazile, J. E., Evans, H. E., & Vanden Berge, J. C. (1993). *Handbook of Avian anatomy: Nomina Anatomica Avium*, second ed. Nuttall Ornithological Club.
- Benito, J., & Olivé, R. (2022). *Birds of the Mesozoic: An Illustrated Field Guide*. Lynx Editions.
- Buscalioni, A. D., & Fregenal-Martínez, M. A. (2010). A holistic approach to the palaeoecology of Las Hoyas Konservat-Lagerstätte (La Huérguina Formation, Lower Cretaceous, Iberian Ranges, Spain). *Journal of Iberian Geology*, 36(2), 297–326. doi: [10.5209/rev_JIGE.2010.v36.n2.13](https://doi.org/10.5209/rev_JIGE.2010.v36.n2.13)
- Buscalioni, A. D., & Poyato-Ariza, F. J. (2016). The wetland of Las Hoyas. In F. J. Poyato-Ariza, & A. D. Buscalioni (Eds.), *Las Hoyas: A Cretaceous wetland* (pp. 232–238). Dr. Friedrich Pfeil Verlag.
- Buscalioni, A. D., Poyato-Ariza, F. J., Marugán-Lobón, J., Fregenal-Martínez, M., Sanisidro, O., Navalón, G., & de Miguel, C. (2016). The wetland of Las Hoyas. In F. J. Poyato-Ariza, & A. D. Buscalioni (Eds.), *Las Hoyas: A Cretaceous wetland* (pp. 238–253). Dr. Friedrich Pfeil Verlag.
- Cambra-Moo, O., Buscalioni, A. D., Cubo, J., Castanet, J., Loth, M.-M., de Margerie, E., & de Ricqlès, A. (2006). Histological observations of enantiornithine bone (Saurischia, Aves) from the Lower Cretaceous of Las Hoyas (Spain). *Comptes Rendus Palevol*, 5(5), 685–691. doi: [10.1016/j.crpv.2005.12.018](https://doi.org/10.1016/j.crpv.2005.12.018)
- Cambra-Moo, O., Buscalioni, A. D., & Delgado-Buscalioni, R. (2008). An approach to the study of variations in early stages of *Gallus gallus* decomposition. *Journal of Taphonomy*, 6(1), 21–40.
- Chiappe, L. M. (1993). Enantiornithine (Aves) tarsometatarsi from the Cretaceous Lecho Formation of northwestern Argentina. *American Museum Novitates*, 3083, 1–27.
- Chiappe, L. M., & Walker, C. A. (2002). Skeletal morphology and systematics of the Cretaceous Euenantiornithes (Ornithothoraces: Enantiornithes). In L. M. Chiappe, & L. M. Witmer (Eds.), *Mesozoic Birds: Above the Heads of Dinosaurs* (pp. 240–267). University of California Press.
- Chiappe, L. M., Marugán-Lobón, J., Ji, S., & Zhou, Z. (2008). Life history of a basal bird: morphometrics of the Early Cretaceous *Confuciusornis*. *Biology Letters*, 4(6), 719–723. doi: [10.1098/rsbl.2008.0409](https://doi.org/10.1098/rsbl.2008.0409)
- Chiappe, L. M., Qingjin, M., Serrano, F., Sigurdson, T., Min, W., Bell, A., & Di, L. (2019a). New Bohaiornis-like bird

- from the Early Cretaceous of China: enantiornithine interrelationships and flight performance. *PeerJ*, 7, e7846. doi: [10.7717/peerj.7846](https://doi.org/10.7717/peerj.7846)
- Chiappe, L. M., Serrano, F., Liu, D., Zhang, Y., & Meng, Q. (2019b). Anatomy and flight performance of the Early Enantiornithine bird *Protopteryx fengningensis*: Information from new specimens of the Early Cretaceous Huajiying Formation of China. *The Anatomical Record*, 303(4), 716–731. doi: [10.1002/ar.24322](https://doi.org/10.1002/ar.24322)
- Chinsamy, A., & Raath, M. (1992). Preparation of fossil bone for histological examination. *Palaeontologia Africana*, 29, 39–44.
- Chinsamy, A., Chiappe, L. M., & Dodson, P. (1995). Mesozoic avian bone microstructure: Physiological implications. *Paleobiology*, 21(4), 561–574. doi: [10.1017/S0094837300013543](https://doi.org/10.1017/S0094837300013543)
- Chinsamy, A., Chiappe, L. M., Marugán-Lobón, J., Chunling G., & Fengjiao, Z. (2013). Gender identification of the Mesozoic bird *Confuciusornis sanctus*. *Nature Communications*, 4, 1381. doi: [10.1038/ncomms2377](https://doi.org/10.1038/ncomms2377)
- Chinsamy, A., Marugán-Lobón, J., Serrano, F., & Chiappe, L. M. (2019). Osteohistology and life history of the basal pygostylian, *Confuciusornis sanctus*. *The Anatomical Record*, 303(4), 949–962. doi: [10.1002/ar.24282](https://doi.org/10.1002/ar.24282)
- Cubo, J., Buscalioni, A. D., Legendre, L. J., Bourdon, E., Sanz, J. L., & de Ricqlès, A. (2022). Palaeohistological inferences of resting metabolic rates in *Concornis* and *Iberomesornis* (Enantiornithes, Ornithothoraces) from the Lower Cretaceous of Las Hoyas (Spain). *Palaeontology*, 65(1), e12583. doi: [10.1111/pala.12583](https://doi.org/10.1111/pala.12583)
- Diéguez, M. C., Martín-Closas, C., Trincao, P., & López-Marrón N. (1995). Palaeontology. Flora. In N. Meléndez (Ed.), *Las Hoyas. A lacustrine Konservat-Lagerstätte, Cuenca, Spain* (pp. 43–49). Universidad Complutense de Madrid.
- Fregenal-Martínez, M., & Meléndez, N. (2016). Environmental reconstruction: a historical review. In F. J. Poyato-Ariza, & A. D. Buscalioni (Eds.), *Las Hoyas: A Cretaceous wetland* (pp. 14–28). Dr. Friedrich Pfeil Verlag.
- Fregenal-Martínez, M., Meléndez, N., Muñoz-García, B., Elez, J., & De la Horra, R. (2017). The stratigraphic record of the Late Jurassic–Early Cretaceous rifting in the Alto Tajo-Serranía de Cuenca region (Iberian Ranges, Spain): genetic and structural evidences for a revision and a new lithostratigraphic proposal. *Revista de la Sociedad Geológica de España*, 30(1), 105–134.
- Hu, D., Li, L., Hou, L., & Xu, X. (2011). A new enantiornithine bird from the Lower Cretaceous of western Liaoning, China. *Journal of Vertebrate Paleontology*, 31, 154–161. doi: [10.1080/02724634.2011.546305](https://doi.org/10.1080/02724634.2011.546305)
- Hu, D., Liu, Y., Li, L., Xu, X., & Hou, L. (2015). *Yuanjiawaornis viriosus*, gen. et sp. nov., a large enantiornithine bird from the Lower Cretaceous of western Liaoning, China. *Cretaceous Research*, 55, 210–219. doi: [10.1016/j.cretres.2015.02.013](https://doi.org/10.1016/j.cretres.2015.02.013)
- Kaye, T. G., Pittman, M., Marugán-Lobón, J., Martín-Abad, H., Sanz, J. L., & Buscalioni, A. D. (2019). Fully fledged enantiornithine hatchling revealed by Laser-Stimulated Fluorescence supports precocial nesting behaviour. *Scientific Reports*, 9, 5006. doi: [10.1038/s41598-019-41423-7](https://doi.org/10.1038/s41598-019-41423-7)
- Knoll, F., Chiappe, L. M., Sánchez, S., Garwood, R. J., Edwards, N. P., Wogelius, R. A., Sellers, W. I., Manning, P. L., Ortega, F., Serrano, F. J., Marugán-Lobón, J., Cuesta, E., Escaso, F., & Sanz, J. L. (2018). A diminutive perinate European Enantiornithes reveals an asynchronous ossification pattern in early birds. *Nature Communications*, 9, 937. doi: [10.1038/s41467-018-03295-9](https://doi.org/10.1038/s41467-018-03295-9)
- Liu, D., Chiappe, L. M., Serrano, F. J., Habib, M., Zhang, Y., & Meng, Q. (2017). Flight aerodynamics in enantiornithines: information from a new Chinese Early Cretaceous bird. *PLoS ONE*, 12(10), e0184637. doi: [10.1371/journal.pone.0184637](https://doi.org/10.1371/journal.pone.0184637)
- Liu, D., Chiappe, L. M., Zhang, Y., Serrano, F. J., & Meng, Q. (2019). Soft tissue preservation in two new enantiornithine specimens (Aves) from the Lower Cretaceous Huajiying Formation of Hebei Province, China. *Cretaceous Research*, 95, 191–207. doi: [10.1016/j.cretres.2018.10.017](https://doi.org/10.1016/j.cretres.2018.10.017)
- Liu, D., Chiappe, L. M., Wu, B., Meng, Q., Zhang, Y., Qiu, R., Xing, H., & Zeng, Z. (2022). Cranial and dental morphology in a bohaiornithid enantiornithine with information on its tooth replacement pattern. *Cretaceous Research*, 129, e105021. doi: [10.1016/j.cretres.2021.105021](https://doi.org/10.1016/j.cretres.2021.105021)
- Martín-Abad, H., & Fregenal-Martínez, M. (2021). The ecology of the Lower Cretaceous coelacanths from Las Hoyas Konservat-Lagerstätte (Cuenca, Spain): A new insight after the integration of palaeontological and sedimentological data. *Spanish Journal of Palaeontology*, 36(2), 191–204. doi: [10.7203/sjp.36.2.21966](https://doi.org/10.7203/sjp.36.2.21966)
- Marugán-Lobón, J., & Vullo, R. (2016). Feathers. In F. J. Poyato-Ariza, & A. D. Buscalioni (Eds.), *Las Hoyas: A Cretaceous wetland* (pp. 190–194). Dr. Friedrich Pfeil Verlag.
- Marugán-Lobón, J., & Chiappe, L. M. (2022). Ontogenetic niche shifts in the Mesozoic bird *Confuciusornis sanctus*. *Current Biology*, 32(7), 1629–1634. doi: [10.1016/j.cub.2022.02.010](https://doi.org/10.1016/j.cub.2022.02.010)
- Marugán-Lobón, J., Chiappe, L. M., Ji, S., Zhou, Z., Chunling, G., Hu, D., & Meng, Q. (2011). Quantitative patterns of morphological variation in the appendicular skeleton of the Early Cretaceous bird *Confuciusornis*. *Journal of Systematic Palaeontology*, 9(1), 91–101. doi: [10.1080/14772019.2010.517786](https://doi.org/10.1080/14772019.2010.517786)
- Morschhauser, E. M., Varricchio, D. J., Chunling, G., Liu, J., Wang, X., Cheng, X., & Meng, Q. (2009). Anatomy of the Early Cretaceous bird *Rapaxavis pani*, a new species from Liaoning Province, China. *Journal of Vertebrate Paleontology*, 29(2), 545–554. doi: [10.1671/039.029.0210](https://doi.org/10.1671/039.029.0210)
- Navalón, G., Marugán-Lobón, J., Chiappe, L. M., Sanz, J. L., & Buscalioni, A. D. (2015). Soft-tissue and dermal arrangement in the wing of an Early Cretaceous bird: Implications for the evolution of avian flight. *Scientific Reports*, 5, 14864. doi: [10.1038/srep14864](https://doi.org/10.1038/srep14864)
- O'Connor, J. K., Chiappe, L. M., Gao, C.-L., & Zhao, B. (2011). Anatomy of the Early Cretaceous enantiornithine bird *Rapaxavis pani*. *Acta Palaeontologica Polonica* 56, 463–475. doi: [10.4202/app.2010.0047](https://doi.org/10.4202/app.2010.0047)
- Sanz, J. L., Bonaparte, J. F., & Lacasa, A. (1988). Unusual Early Cretaceous bird from Spain. *Nature*, 331, 433–435. doi: [10.1038/331433a0](https://doi.org/10.1038/331433a0)
- Sanz, J. L., Chiappe, L. M., & Buscalioni, A. D. (1995). The osteology of *Concornis lacustris* (Aves: Enantiornithes) from the Lower Cretaceous of Spain and a reexamination of its phylogenetic relationships. *American Museum Novitates*, 3133, 1–23.
- Sanz, J. L., Pérez-Moreno, B., Buscalioni, A. D., Moratalla, J. J., Ortega, F., & Poyato-Ariza, F. J. (1996). An Early

- Cretaceous bird from Spain and its implications for the evolution off light. *Nature*, 382, 442–445. doi: [10.1038/382442a0](https://doi.org/10.1038/382442a0)
- Sanz, J. L., Chiappe, L. M., Fernández-Jalvo, Y., Ortega, F., Sánchez-Chillón, B., Poyato-Ariza, F. J., & Pérez-Moreno, B. (2001). A Cretaceous pellet. *Nature*, 409, 98–99. doi: [10.1038/35059172](https://doi.org/10.1038/35059172)
- Sanz, J. L., Chamero, B., Chiappe L. M., Marugán-Lobón, J., O'Connor, J. K., Ortega, F., & Escaso, F. (2016). Aves. In F. J. Poyato-Ariza, & A. D. Buscalioni (Eds.), *Las Hoyas: A Cretaceous wetland* (pp. 183–189). Dr. Friedrich Pfeil Verlag.
- Serrano, F. J., Chiappe L. M., Palmqvist, P., Figueirido, B., Marugán-Lobón, J., & Sanz, J. L. (2018). Flight reconstruction of two European enantiornithines (Aves, Pygostylia) and the achievement of bounding flight in Early Cretaceous birds. *Palaeontology*, 61(3), 359–368. doi: [10.1111/pala.12351](https://doi.org/10.1111/pala.12351)
- Vicente, A., & Martín-Closas, C. (2013). Lower Cretaceous charophytes from the Serranía de Cuenca, Iberian chain: taxonomy, biostratigraphy and palaeoecology. *Cretaceous Research*, 40, 227–242. doi: [10.1016/j.cretres.2012.07.006](https://doi.org/10.1016/j.cretres.2012.07.006)
- Wang, M., Zhou, Z. H., O'connor, J. K., & Zelenkov, N. V. (2014a). A new diverse enantiornithine family (Bohaiornithidae fam. nov.) from the Lower Cretaceous of China with information from two new species. *Vertebrata Palasiatica*, 52, 31–76.
- Wang, M., Zhou, Z., & Xu, G. (2014b). The first enantiornithine bird from the Upper Cretaceous of China. *Journal of Vertebrate Paleontology*, 34(1), 135–145. doi: [10.1080/02724634.2013.794814](https://doi.org/10.1080/02724634.2013.794814)
- Wang, M., Li, D., O'Connor, J. K., Zhou, Z., & You, H. (2015). Second species of enantiornithine bird from the Lower Cretaceous Changma Basin, northwestern China with implications for the taxonomic diversity of the Changma avifauna. *Cretaceous Research*, 55, 56–65. doi: [10.1016/j.cretres.2015.01.008](https://doi.org/10.1016/j.cretres.2015.01.008)
- Wang, M., & Zhou, Z. (2017). A morphological study of the first known piscivorous enantiornithine bird from the Early Cretaceous of China. *Journal of Vertebrate Paleontology*, 37(2), e1278702. doi: [10.1080/02724634.2017.1278702](https://doi.org/10.1080/02724634.2017.1278702)
- Zhang, F., & Zhou, Z. (2000). A primitive enantiornithine bird and the origin of feathers. *Science*, 290, 1955–1959. doi: [10.1126/science.290.5498.1955](https://doi.org/10.1126/science.290.5498.1955)
- Zhang, F., Zhou, Z., Hou, L., & Gu, G. (2001). Early diversification of birds: Evidence from a new opposite bird. *Chinese Science Bulletin*, 46, 945–949. doi: [10.1007/BF02900473](https://doi.org/10.1007/BF02900473)
- Zhang, F., Ericson, P. G. P., & Zhou, Z. (2004). Description of a new enantiornithine bird from the Early Cretaceous of Hebei, northern China. *Canadian Journal of Earth Sciences*, 41(9), 1097–1107. doi: [10.1139/e04-055](https://doi.org/10.1139/e04-055)
- Zhang, Y., O'Connor, J. K., Liu, D., Meng, Q., Sigurdson, T., & Chiappe, L. M. (2014). New information on the anatomy of the Chinese Early Cretaceous Bohaiornithidae (Aves: Enantiornithes) from a subadult specimen of *Zhouornis hani*. *PeerJ*, 2, e407. doi: [10.7717/peerj.407](https://doi.org/10.7717/peerj.407)
- Zhou, Z. H., & Hou, L. H. (2002). The discovery and study of Mesozoic birds in China. In L. M. Chiappe, & L. Witmer (Eds.), *Mesozoic Birds: Above the Heads of Dinosaurs* (pp. 160–183). University of California Press.
- Zhou, Z., Clarke, J., & Zhang, F. (2008). Insight into diversity, body size and morphological evolution from the largest Early Cretaceous enantiornithine bird. *Journal of Anatomy*, 212, 565–577. doi: [10.1111/j.1469-7580.2008.00880.x](https://doi.org/10.1111/j.1469-7580.2008.00880.x)
- Zhang, Z., Chiappe, L. M., Han G., & Chinsamy, A. (2013). A large bird from the Early Cretaceous of China: new information on the skull of enantiornithines. *Journal of Vertebrate Paleontology*, 33(5), 1176–1189. doi: [10.1080/02724634.2013.762708](https://doi.org/10.1080/02724634.2013.762708)

